TEORIISKA I PRIMENJENA MEHANIKA 14 pp. 103–115, 1988, UDK 533.6

CALCULATION OF 2–D TRANSONIC FULL POTENTIAL EQUATION WITH FINITE ELEMENT METHOD

Z. I. Petrović, S. N. Stupar

(Received 12. 05. 1988)

Introduction

Much of the research attention is paid to transonic flow calculations during last fifteen years. Physical laws which describe such flow are governed with elliptic--hyperbolic partial differential equations, with unknown, in advance position of hyperbolic region. For typical transonic flow hyperbolic region correspond to supersonic pocket surrounded with subsonic flow which correspond to elliptic region. Transition to subsonic from supersonic flow is abrupt through shock wave, which position is also unknown.

Because of complexity of calculation of such flows, high performance computers are needed, and governing equation simplifications must be done. Simplification of governing equations can be done by neglecting some of less important fluid characteristics. It is common approximation that in order to determinate lift force fluid viscosity can be neglected. For small angles of attack, this simplification gives good results. Besides that, flight with high angles of attack and with strong shock waves is avoided in practice, so small intensity shock waves are accepted, and isentropic assumption can be allowed in this case.

It can be shown that for small angles of attack assumption of small vorticity can be imposed. Flows which would be presented in this work can be declared as inviscid flow with weak shock waves or compressible potential flows.

Existence of the velocity potential is direct consequence of vorticity negligence. Existence of lift is directly connected with circulation, which is the consequence of vorticity. In order to obtain meaningful results coordinate cut, which connects outer boundary with airfoil, must be introduced. Such cut is an additional boundary on which some boundary conditions must be defined.

Governing Equations

Governing equations for inviscid irrotational flow can be obtained form Euler equations, which are generally [1] expressed:

$$\frac{\partial}{\partial t}\oint_V \rho\, dV + \oint_S \rho\, \vec{V}\cdot d\vec{S} = 0 \qquad \text{Continuity equation} \qquad (1)$$

Differential form of Continuity equation (1) is:

$$\frac{\partial \rho}{\partial t} + \nabla \cdot (\rho \vec{V}) = 0. \tag{2}$$

Momentum equation in integral form can be expressed:

$$\frac{\partial}{\partial t} \oint_V \rho \vec{V} dV + \oint_S (\rho \vec{V} \cdot d\vec{S}) \vec{V} = - \oint_S p d\vec{S} + \oint_V \rho \vec{f} dV \text{ Momentum eq.} \tag{3}$$

Differential form of momentum equation (3), can be presented:

$$\rho \frac{D\vec{V}}{Dt} = -\nabla p + \nabla \rho.$$

Integral form of Energy equation can be given with:

$$\frac{\partial}{\partial t} \oint_V \rho (e + \vec{V}^2/2) dV + \oint_S \rho (e + V^2/2) \vec{V} \cdot d\vec{S} = \oint_V \dot{q} \rho \, dV - \oint_S p \vec{V} \cdot d\vec{S} + \oint_V \rho (\vec{f} \cdot \vec{V}) dV \tag{4}$$

while associated differential form of former equation is:

$$\rho \frac{D(e + V^2/2)}{Dt} = \rho \dot{q} - \nabla \cdot (p\vec{V}) + \rho (\vec{f} \cdot \vec{V}) \tag{5}$$

Equation of state and internal energy definition is given below:

$$p = \rho RT,$$

$$e = c_v T.$$

Equations (1) to (5) are very hard to solve for general case, and for solution of such equations appropriate computer is needed. It is common case, therefore, to add some of following equations to equations mentioned before in order to simplify problem:

$$\vec{\zeta} = \nabla \times \vec{V} = 0, \tag{6}$$

or equivalently:

$$\vec{V} = \nabla \cdot \Phi,$$

equation for isentropic state change:

$$\frac{p}{p_0} = \left(\frac{\rho}{\rho_0} \right)^k. \tag{7}$$

In this way we have artifically increased the number of equations which can be used to describe transonic flows. Some of physical laws can be avoided when some of additional equations are used. Introduced simplifications, velocity potential equation (6) and isentropic flow assumption (7), restrict applicability of obtained solutions on irrotational flows and flows with weak shock waves, without flow separation.

Equations which describe such flows are:

$$\nabla \cdot (\rho \nabla \cdot \Phi) = 0, \tag{8}$$

and

$$\rho = \left[1 - \frac{k-1}{2} M_\infty^2 \left((\nabla \Phi)^2 - 1 \right) \right]^{\frac{1}{k-1}}. \tag{9}$$

Equations (8) and (9) are normalized with undisturbed magnitudes of fluid velocity (U_∞ and density ρ_∞).

Boundary conditions

In order to determine circulation around airfoil with velocity potential formulation it is necessary to make calculation on simply connected domain. This can be done with cut through computational domain as it is shown on Fig. (1)

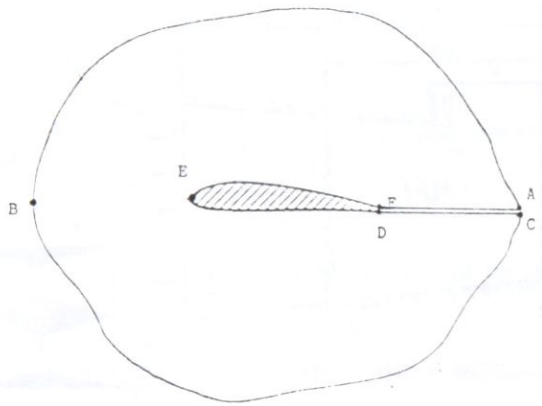

Figure 1: Simply connected domain around the airfoil

Boundary conditions on the airfoil surface should express its impermeability:

$$\frac{\partial \Phi}{\partial n} = 0, \tag{10}$$

which can be otherwise stated that normal component of the velocity on airfoil contour is zero. Undisturbed conditions can be specified on the far filed boundary t.e.:

$$\Phi = u_\infty x + v_\infty y \tag{11}$$

Part of boundary contour which belongs to cut is neither solid surface nor far field boundary, for which undisturbed conditions can be specified. For specification of boundary conditions on this part of contour "$2n$" additional conditions should be specified for each "n" couple points on the cut. First "n" conditions can be specified by treating these points as ordinary points of computational domain. sAdditional "n" conditions are supplied based on the fact that potential on the cut thould have jump equal to the magnitude of the circulation Γ around the airfoil, his additional "n" equations can be expressed in the following form:

$$\Phi_d = \Phi_g + \Gamma. \tag{12}$$

In the equation (12) remains undertermined magnitude of the circulation Γ, which should be obtained from Kutta—Joukowsky condition. For numerical calculations this condition can be expressed as requirement for speed equality on the upper and lower surface of the airfoil near the trailing edge:

$$|\nabla \Phi|_u = |\nabla \Phi|_l. \tag{13}$$

Where subscripts "u" and "l" denote flow parameters on the upper and lower surface of the airfoil near the trailing edge, respectively.

Artificial compressibility method

In order to simulate flow with shock waves with isentropic equation mass assessment in the supersonic region of the computational domain is necessary, [2]. This fact can be simply explained considering Fig. (2).

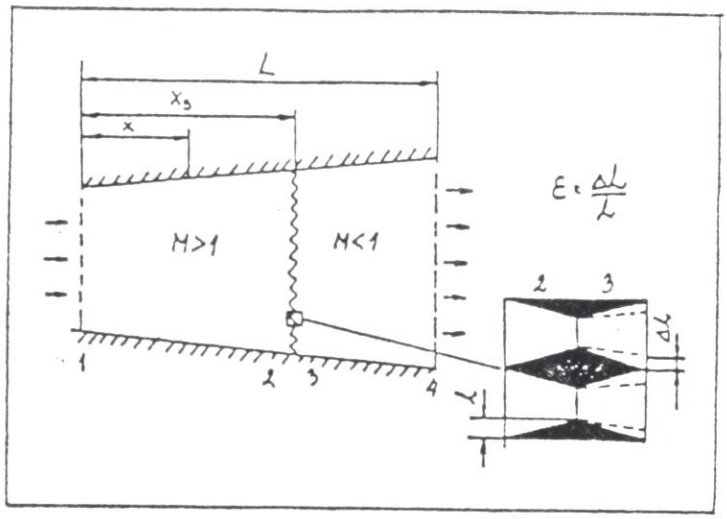

Figure 2: Transonic flow through nozzle

If we substitute shock wave in the divergent part of the nozzle on Figure (2) with row of convergent – divergent nozzles, than isentropic simulation of the shock wave is obtained. Flow characteristics should be the same after passing this nozzles as they are after real shock wave. This is, of course, impossible, but how good shock wave can be simulated with this concept, is the question which should be answered. If the correct exit pressure should be simulated then much smaller exit area of the nozzles should be then it actually is, so mass should be added to simulate after shock pressure. Good pressure simulation is necessary for proper lift force calculation.

Mass assessment in supersonic flow region can be obtained by application of artificial compressibility method [3], by which density in the supersonic flow region is modified on the following way:

$$\tilde{\rho} = \rho - \mu \frac{\partial \rho}{\partial S} \Delta_s \tag{14}$$

switching function μ (different from zero only in the supersonic flow domain), is defined:

$$\mu = \alpha \cdot \max(0, 1 - 1/M^2), \qquad \alpha \approx 1.0. \tag{15}$$

Finite element formulation of the flow problem

In this work linear, quadrilateral, isoparametric finite elements are used. Smaller elements are used in the domain where gradients of flow parameters where bigger, Figure (3), in the remaining part of the computational domain greater elements where used.

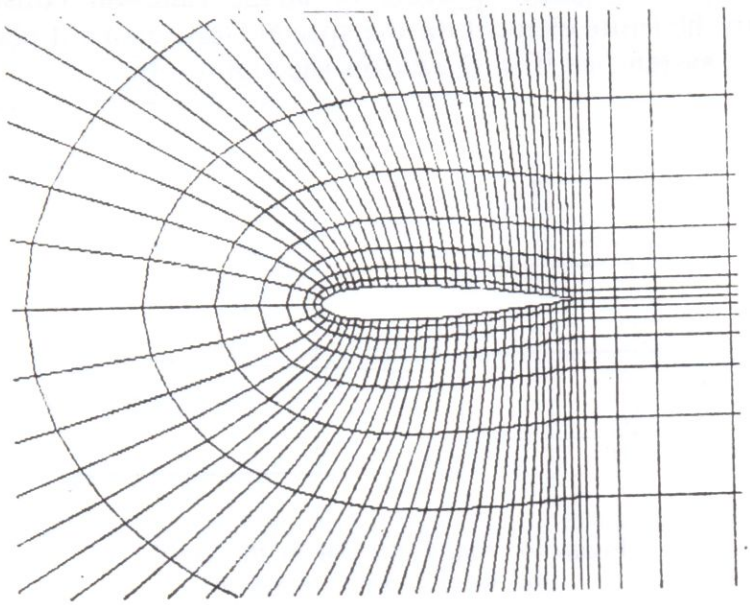

Figure 3: Typical composition of smaller and bigger F. E.

Value of the velocity potential over the finite elements is determined by interpolation:

$$\tilde{\Phi}(x, y) = \sum_{i=1}^{4} N_i(x, y) \cdot \tilde{\Phi}_i, \tag{16}$$

with $\sim$ in equation (16) approximate values of velocity potential are assigned, while with $N_i(x, y)$ are interpolating polynomials signed, with which approximate value of the velocity potential are calculated over finite element. With Φ_i the value of velocity potential at node "i" is signed.

If approximate values of velocity potential are substituted in equation (8) error for each point of computational domain will be obtained as a discrepancy from exact solution. Error of approximation is function of the point on the computational domain, if it is multiplied with shape function and summed over computational domain and minimum of such value is found by differentiating error with unknown values of velocity potential, classical Galerkin procedure is obtained:

$$\iint_S N_i(x, y) [\nabla (\tilde{\rho} \nabla \Phi)] \, dx \, dy = \varepsilon, \tag{17}$$

or:

$$\iint_S \left(\frac{\partial N_i(x, y)}{\partial x} \tilde{\rho} \frac{\partial \Phi}{\partial x} + \frac{\partial N_i(x, y)}{\partial y} \tilde{\rho} \frac{\partial \Phi}{\partial y} \right) dx \, dy - \oint \tilde{\rho} N_i(x, y) \frac{\partial \Phi}{\partial n} \, dG = 0 \tag{18}$$

Integration over whole computational domain can be split on sequence of separate finite element integrations, what introduce in equation (18) symbol Σ in front of the integral, while integration remains only over the area of the element. Line integral should be calculated in the case that the boundary of the element overlaps with the computational domain boundary.

Arbitrary position of thef inite element the in the computational domain, as well its arbitrary orientation makes process of shape function construction harder. It is usual to map the finite element on the special finite element placed in the origin of the coordinate system, as it is shown on the figure (4).

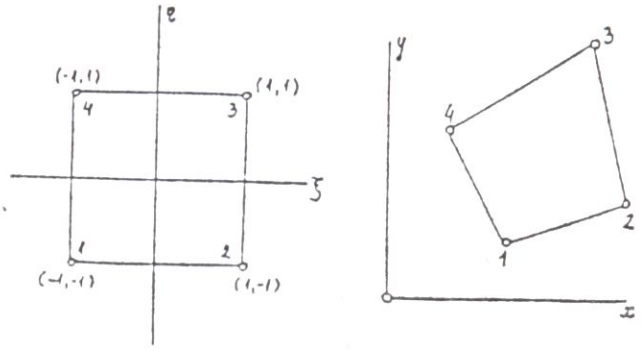

Figure 4: Finite element in the global and local coordinate system

For mapping local shape functions are used, coordinate of arbitrary point within the element can be determined:

$$x = \sum_{i=1}^{4} N_i(\xi, \eta) \cdot x_i,$$

$$y = \sum_{i=1}^{4} N_i(\xi, \eta) \cdot y_i \tag{19}$$

Shape functions, $N_i(\xi, \eta)$, for the case of linear quadrilateral elements are defined:

$$N_i(\xi, \eta) = (1 + \xi_i \xi)(1 + \eta_i \eta)/4,$$

while the derivatives of the shape functions in local coordinate system are:

$$\frac{\partial N_i}{\partial \xi} = \xi_i \cdot (1 + \eta_i \eta)/4,$$

$$\frac{\partial N_i}{\partial \eta} = (1 + \xi_i \xi) \cdot \eta_i/4.$$

If coordinates ξ, μ are substituted in equation (18) then it is necessary to calculate Jacobean of the transformation:

$$[J^e] = \begin{bmatrix} \frac{\partial x}{\partial \xi} & \frac{\partial y}{\partial \xi} \\ \frac{\partial x}{\partial \eta} & \frac{\partial y}{\partial \eta} \end{bmatrix} = \begin{bmatrix} \frac{\partial N_1}{\partial \xi} & \frac{\partial N_2}{\partial \xi} & \frac{\partial N_3}{\partial \xi} & \frac{\partial N_4}{\partial \xi} \\ \frac{\partial N_1}{\partial \eta} & \frac{\partial N_2}{\partial \eta} & \frac{\partial N_3}{\partial \eta} & \frac{\partial N_4}{\partial \eta} \end{bmatrix} \cdot \begin{bmatrix} x_1 & y_1 \\ x_2 & y_2 \\ x_3 & y_3 \\ x_4 & y_4 \end{bmatrix}$$

With calculated value of the Jacobean it is possible to calculate derivatives of shape function in global coordinate system:

$$\begin{Bmatrix} \frac{\partial N_i}{\partial x} \\ \frac{\partial N_i}{\partial y} \end{Bmatrix} = [J^e]^{-1} \cdot \begin{Bmatrix} \frac{\partial N_i}{\partial \xi} \\ \frac{\partial N_i}{\partial \eta} \end{Bmatrix}.$$

Elementary area in global coordinate system can be calculated using area in the local coordinate system according to:

$$dx\,dy = |J^e|\,d\xi\,d\eta,$$

where $|J^e|$ is determinant of the Jacobean. With sign $[B]$ we shall consider the following matrix:

$$[B] = \begin{bmatrix} \frac{\partial N_1}{\partial \xi} & \frac{\partial N_2}{\partial \xi} & \frac{\partial N_3}{\partial \xi} & \frac{\partial N_4}{\partial \xi} \\ \frac{\partial N_1}{\partial \eta} & \frac{\partial N_2}{\partial \eta} & \frac{\partial N_3}{\partial \eta} & \frac{\partial N_4}{\partial \eta} \end{bmatrix}$$

Contribution of the single finite element to the global coefficient matrix, equation (18), after substitution of shape functions to equation (18) is obtained:

$$\int_{-1}^{1}\int_{-1}^{1} [B]^T \tilde{\rho}\,[B]\,d\xi\,d\eta\,\{\Phi\} - \int_{Ge} \tilde{\rho}\,\{N\}\left\{\frac{\partial \Phi}{\partial \eta}\right\} dG_e \qquad (20)$$

with G_e is designed side of the finite element which belongs to boundary of computational domain, while with $\{\Phi\}$ is designed vector of nodal values of velocity potential:

$$\{\Phi\} = \begin{Bmatrix} \Phi_1 \\ \Phi_2 \\ \Phi_3 \\ \Phi_4 \end{Bmatrix}$$

Under assumption that without great error density ρ over finite element can be considered constant, it is possible to put density in front of the integral in the equation (20), so that contribution of the finite element after numerical integration is:

$$\tilde{\rho}_e\,[K^e]\,\{\Phi\} - \tilde{\rho}_e\,\{f\} \qquad (21)$$

Implementation of artifical compressibility method

Artificial compressibility concept is given with equation, (14), in which following expression should be determined:

$$\frac{\partial \rho}{\partial S} \nabla_s \tag{22}$$

This expression is substituted with density difference between density of the current finite element and the upstream density. Upstream density is determined from the densities of the upstream finite elements, as it is shown on the figure (5). Expression given with equation (22) is approximated with density difference:

$$\rho - \rho_-$$

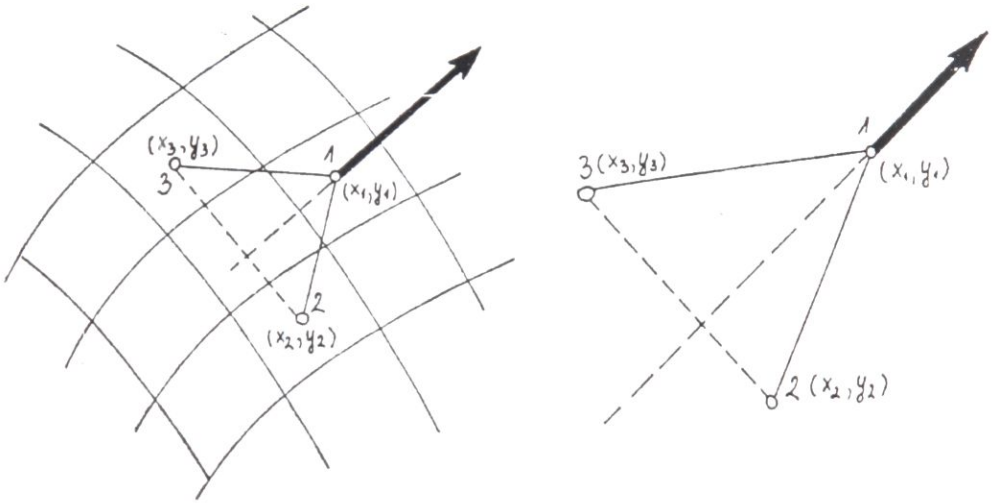

Figure 5: Density ρ- is taken from the point obtained by intersecting line which connect „middle" of two upstream elements and line which pass through „middle" point of the current element and is parallel with velocity at that point.

Summing up what is mentioned, density $\tilde{\rho}$ is calculated on the following way:

$$\tilde{\rho} = \rho - \mu(\rho - \rho_-) \tag{23}$$

Equations which describe such flows are nonlinear partial differential equation of mixed elliptic-hyperbolic type, with line of the discontinuity of flow parameters, and with unknown position of hyperbolic region. This equations can be solved only iteratively. Solution procedure should provide mechanism for proper positioning of shock wave in the computational domain.

If, during the solution process, is found that position of the shock wave is incorrect points just before and just after the shock wave should be treated in a such way that shock wave is moved to the proper place.

To explain process of proper shock wave position determination with finite element method, model of quasi one dimensional flow is used and from the equation for flow rate [4]:

$$\dot{m} = \rho A V,$$

where A is channel cross section, and V is stream velocity through channel, with $\dot{m}$ flow rate is disegnated. It is easy to obtain function $\dot{m}/A$ as a function of Mach number only:

$$\frac{\dot{m}}{A} = \rho V = \rho \sqrt{kp/\rho}\, \frac{V}{\sqrt{kp/\rho}} = \sqrt{k \rho p} \cdot M.$$

Dividing quantities under square with $\rho_0 p_0$ following relations are obtained for p/p_0 and ρ/ρ_0:

$$\frac{\dot{m}}{A} = \sqrt{k \rho_0 p_0} \cdot \left(\frac{p}{p_0}\, \frac{\rho}{\rho_0}\right)^{\frac{1}{2}} \cdot M,$$

These relations can be simply obtained as a function of Mach number using the assumption that flow is isentropic:

$$Q = \frac{\dot{m}}{A\sqrt{k \rho_0 p_0}} = \frac{M}{\left(1 + \frac{k-1}{2} M^2\right)^{\frac{k+1}{2(k-1)}}} \tag{24}$$

Relation between Mach numbers before and after shock wave, (M_1) and (M_2), is given with equation for the channel flow

$$M_2^2 = \frac{(k-1) M_1^2 + 2}{2kM_1^2 - (k-1)}, \tag{25}$$

Functional dependence of mass flow rate on Mach number, M, is shown on the figure (6), on which two points are separated. Point with assigned number 1 is just before shock wave while point 2 is just after the shock wave. This diagram is obtained by calculation of reduced flow rate, Q, with equation (24), for $M>1$,

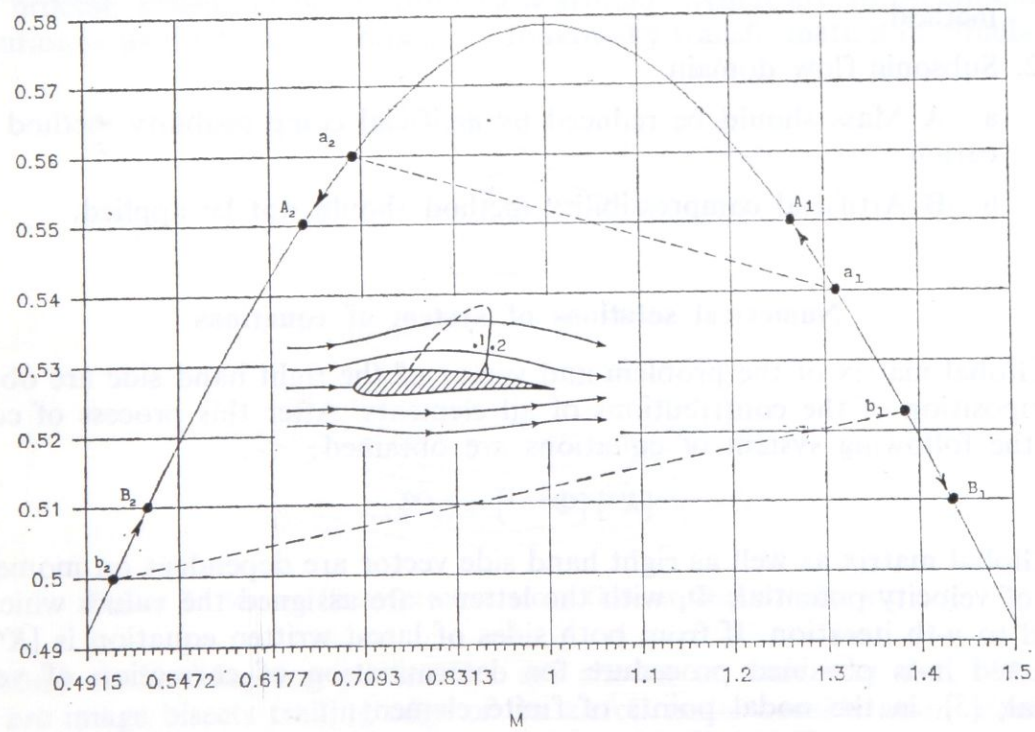

Figure 6: Diagram of flow rate Mach number dependence

subsonic Mach number is calculated with equation (25). Calculation of quantity Q for $M<1$ would not give proper result because total pressures with which flow rate is divided is different for points before and after shock wave.

With symbols a_1 and a_2 are assigned values of Mach number and mass flow rate for the case when mass flow rate in the subsonic domain is greater than mass flow rate in supersonic domain. With symbols b_1 and b_2 are assigned points which correspond to opposite case, t.e. when mass flow in the subsonic flow domain is smaller than the mass flow rate in the supersonic flow domain.

Analyzing equations (24) and (25) the following conclusion can be made:

$$\left|\frac{dQ}{dM}\right|_2 > \left|\frac{dQ}{dM}\right|_1 \tag{26}$$

If balanced mass flow rates from diagram (6) are assigned with A_1—A_2 and B_1—B_2, and taking into account:

$$\tilde{\rho} = \rho - \mu \cdot (\rho - \rho_-)$$

it is obtained that $\tilde{\rho}$ is greater from locally calculated density ρ for the case $\rho<\rho_-$, and smaller for the case $\rho>\rho_-$. From this consideration it is clear that application of artificial compressibility method assess mass in the supersonic part of computational domain while in the subsonic flow domain mass is reduced.

In order to balance mass flow rate from diagram (6) the following should be made:

1. Supersonic flow domain.

   a—A Application of artificial compressibility method increase mass in the supersonic flow domain.

   b—B Mass should be reduced by application of artificial compressibility method.

2. Subsonic flow domain.

   a—A Mass should be reduced by artificial compressibility method application.

   b—B Artificial compressibility method should not be applied.

Numerical solutions of system of equations

Global matrix of the problem and vector of the right hand side are obtained by composition of the contributions of all elements. After this process of composition the following system of equations are obtained:

$$[K^n]\{\Phi^{n+1}\} = \{f^n\}.$$

Global matrix as well as right hand side vector are dependent on momentous values of velocity potential, Φ, with the letter n are assigned the values which correspond to n-th iteration. If from both sides of latest written equation is $[K^n]\{\Phi^n\}$ substracted it is obtained procedure for determination of correction of velocity potential, [5], in the nodal points of finite element:

$$[K^n] \triangle \{\Phi\} = -\beta([K_n]\{\Phi^n\} - \{f^n\}), \tag{27}$$

where $\Delta\Phi$ is defined:

$$\Delta\Phi = \Phi^{n+1} - \Phi^n,$$

Coefficient β is compensating coefficient, which task is to slow down changes of the right side vector of the equation (27). Equation (27) is suitable for non circulatory flows, t.e. when there are no functional relations between points on the computational domain boundary. But for flows, such as flow around airfoil, for which exists cut through computational domain and for which values of the potential on the upper and lower surface are mutually dependent, iteration procedure should be modified. This dependence, when Galerkin procedure and Lagrangian multiplier method is applied, yields to global matrix with zeroes on the main diagonal, what is not acceptable for the great number of unknowns.

In this work it will be shown alternative way for imposition of additional conditions for the case of circulatory flow around airfoil. For this special case aditional conditions are expressed with equation (12). Unknown value of velocity potential is split on two parts, [6]:

$$\Phi = \Phi_1 + \Phi_2;$$

For the second part of velocity potential Φ_2 is chosen function which statisfies conditions (12) and for which magnitude of circulation is parameter, with which potential jump on the cut is defined. For such function can be chosen solution of flow equation for point vortex which is:

$$\Phi_2 = \Gamma \arctan\left(\frac{y\sqrt{1-M_\infty^2}}{x}\right).$$

In the upper equation is it supposed that cut through computational domain overlaps with $x-$axis. Calculations done by authors are shown that point vortex introduce in computational procedure high gradients which locally destabilises solution process. Instead of point vortex flow around circular arc airfoil circulatory flow solution is used which is obtained by Joukowsky transformation of circulatory

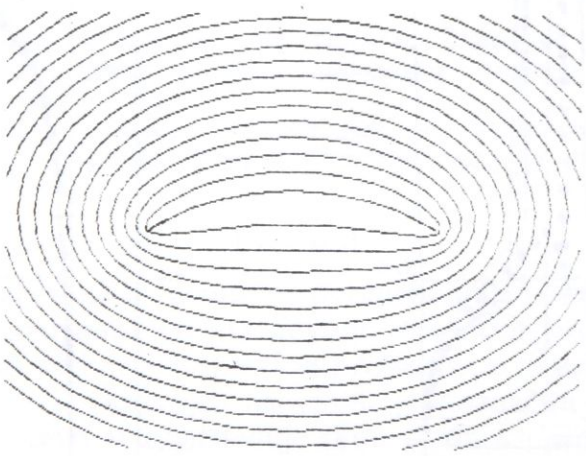

Figure 7: Stream lines for circulatory flow around circular arc

flow around circle. Mapping parameters are chosen in such way that obtained circular arc image bisects trailing edge of the airfoil under consideration. Example of circulatory flow around circular arc is shown with figure (7).

Value of the circulation Γ is determined from the velocity equality at the trailing edge of the airfoil. This condition expressed through formulae is:

$$\Gamma^{n+1} = \Gamma^n + b\,(u_d^2 - u_g^2), \tag{28}$$

purpose of the parametar δ, is to slow down abrupt changes of the circulation Γ, to avoid computational instabilities.

After spilitting of velocity potential on two functions equation (27) can be written:

$$[K^n]\,\Delta\{\Phi_2\} = -\beta\,([K^n]\{\Phi_1^n + \Phi_2^n\} - \{f^{n+1}\} + \Gamma^n\{g^n\}), \tag{29}$$

with $[g^n]$ is taken contribution of function which simulate circulatory flow around circular arc, in this contribution only densities are dependent on number of iteration n.

Examples of calculation

Diagram of pressure coefficient distribution over airfoil chord for Mach number $M=0{,}8$ and $\alpha=0$, heavy dots, is shown on the figure (8) on the diagram on which are shown results for few other well known programs for calculation of transonic flows, [7]:

Pressure coefficient diagram for Mach number $M=0.85$ and $\alpha=0$ is shown on figure (9).

Typical diagram of convergence history is shown on figure (10).

Izo—Mach lines for subsonic part of flow domain is shown on figure (11) for $M=0.85$ and $\alpha=1$.

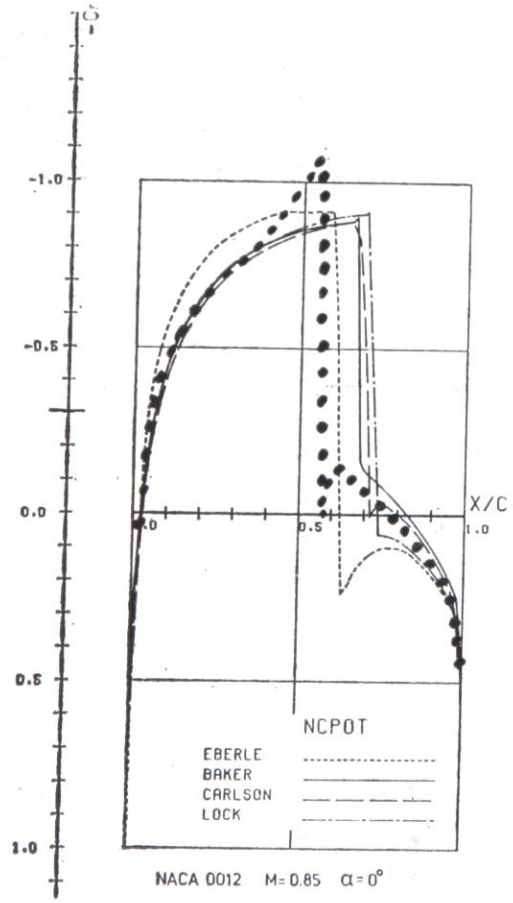

Figure 8: Pressure coefficient distribution *Cp*, for $M=0.8$ and $\alpha=0$.

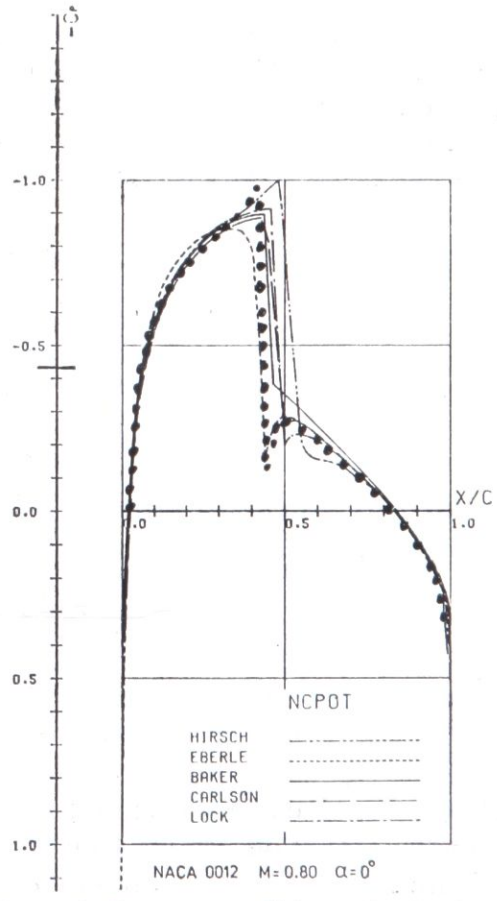

Figure 9: Pressure coeficient distribution, *Cp*, for $M=0.85$ and $\alpha=0$.

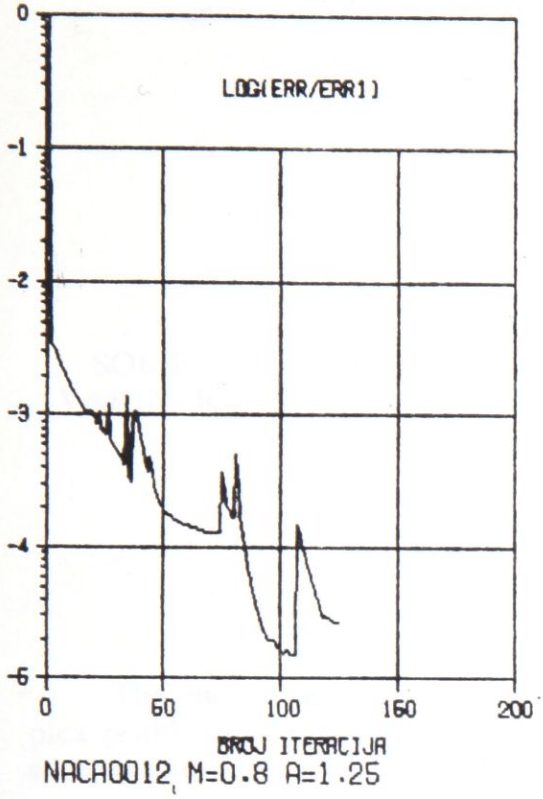

Figure 10: Convergence history diagram

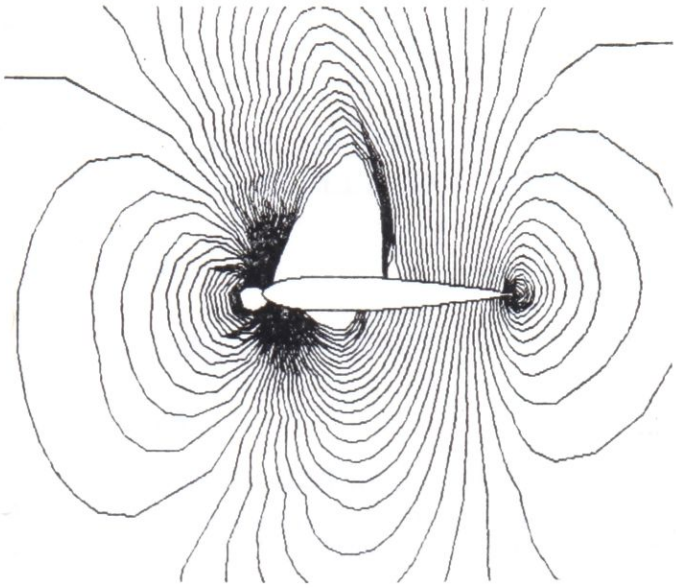

Figure 11: Izo—Mach lines for $M_\infty = 0.85$ and $\alpha = 1$.

REFERENCES

[1] John D. Anderson, Jr., *Fundamentals of Aerodynamics*, McGraw—Hill International Editions, McGraw-Hill Book Co., New York, 1984.

[2] R. Gregg and P. Henne, *An Assesment of Mass Conservation for Potential Flow Shock Simulation*, AIAA-82-0158, AIAA 20th Aerospace Sciences Meeting, Jan. 11—14, 1982.

[3] M. Hafez, J. South and E. Murman, *Artificial Compressibility Methods for Numerical Solutions of Transonic Full Potential Equation*, Vol. 17, No. 8, Novembar 1982.

[4] E. L. Houghton and A. E. Brock, *Tables for the Compressible Flow of Dry Air*, Edvard Arnold, London, 1975.

[5] W. G. Habashi, *Advances in Computational Transonic*, Pineridge Press, London, 1985.

[6] Z. Petrović, *Doprinos numeričkim rešenjima transoničnog strujanja*, Doktorska disertacija, Mašinski Fakultet Beograd, 1986.

[7] A. Rizzi and H. Viviand, *Numerical Methods for the Computation of Inviscid Transonic Flows with Shock faves*, Friedrich Viweg & Sohn, Braunschweig, Wiesbaden, 1981.

Izvod

U ovom radu razmatra se proračun potencijalnog dvodimdnzionog transoničnog strujanja diskretizovanog Galerkinovom metodom preko konačnih elemenata. Metod veštačke kompresibilnosti je primenjen u nadzvučnom delu strujnog polja. Potencijal brzine je razdvojen na jednu jepnoznačnu funkciju i na jednu višeznačnu funkciju, kojom se obezbeđuje skok vrednosti potencijal na mestu reza u strujnom polju. Diskretizovano strujno polje je rešavano iterativnim putem, za koji je dat algoritam proračuna. Za aeroprofil NACA0012 dati su rezultati proračuna strujanja za tipične transonične Mahove brojeva $M = 0{,}8$ i $M = 0.86$ u obliku raspodele koeficijenta pritiska oko aeroprofila.

Mašinski Fakultet
Beograd
27. marta 80